SURVEYORS, GPS AND THE
WORLD SAILING SPEED RECORD

R.E. Deakin, W.N. Cameron, D.M. Silcock and K. Zhang

Department of Geospatial Science
RMIT University
GPO Box 2476V
MELBOURNE VIC 3001

ABSTRACT

The highest recorded speed reached by any craft under sail is 46.52 knots (86 km/h). This record was set at Shallow Inlet Victoria in 1993 by Simon McKeon and Tim Daddo sailing the yacht *Yellow Pages Endeavour;* a triplanar wing sail yacht, designed and constructed in Australia. In 2002, they will attempt to raise the record above 50 knots with a new yacht, *Macquarie Innovation,* an improved version of *Yellow Pages Endeavour.* To determine the speed the Macquarie team has developed their own low-tech approach using a digital video recorder aboard the yacht and sighting posts at fixed distances on shore. With the latest development of GPS technology, speed and distance travelled can be measured in an efficient and precise manner and this paper compares both techniques on simulated runs of the yacht before a recent record attempt.

INTRODUCTION

World Sailing Speed Records are awarded by the World Sailing Speed Record Council (WSSRC 2002), an affiliated body of the International Sailing Federation (ISAF 2002). Eligible records are average velocities over a 500-metre course by a yacht whose only method of propulsion is the natural action of the wind on the sail. A record will only be ratified if the attempt has been monitored by a commissioner appointed by the ISAF/WSSRC. The course may be defined by floats on the water or by transit posts on shore and a timed run is the difference between start and finish times recorded to the nearest one hundredth of a second. Speed, distance divided by time, is calculated to the nearest one hundredth of a knot with allowance made for the resolved component of any tidal stream and/or current flow on the course. A course is deemed unsuitable if the tidal flow and/or current exceed one knot.

World Sailing Speed Records (WSSRC 2002) are established in sail area divisions:
   10 Sq. m Class: up to and including 10 m^2
   A Class: from 10 m^2 up to and inc. 150 square feet (13.94 m^2)
   B Class: from 150 square feet up to and inc. 235 square feet (21.83 m^2)
   C Class: from 235 square feet up to and inc. 300 square feet (27.87 m^2)
   D Class: over 300 square feet

The fastest of these class records also becomes the outright World Sailing Speed Record.

In 1993 at Shallow Inlet, Simon McKeon and Tim Daddo, sailing the triplanar wing sail yacht *Yellow Pages Endeavor,* captured the B, C and D Class World Sailing Speed Records on the way to recording the highest speed ever attained by any craft under sail of 46.52 knots. They achieved these multiple records by adjusting the area of the wing sail between runs. *Yellow Pages Endeavour* was designed and constructed by Lindsay Cunningham and raced by a group of volunteers. In March this year, the group, now known as the Macquarie World Speed Sailing Team attempted to raise their own record above 50 knots with a new yacht *Macquarie Innovation.* This yacht, an improvement on *Yellow Pages*

Endeavour, is a solid wing sail attached by aerofoil sections to three small pontoons, one of which contains the skipper and crew. In the right wind and sea conditions, with the skipper steering and the crew trimming the wing sail, the crew pod lifts clear of the water and the yacht rises slightly, planing on the pontoons. Small hydrofoils under the pontoons assist the hull planing and offer side force resistance as well as steering since control from the front pontoon.

Both *Macquarie Innovation* and *Yellow Pages Endeavour* are developments of the speed potential exhibited by C Class catamarans, the yachts that contest the Little America's Cup – a challenge cup, like the America's Cup, where a sailing club challenges the cup holder (another sailing club) to a series of match races. McCrae Yacht Club on Port Phillip Bay, Victoria won the cup in 1985 with *Victoria-150* and defended it successfully until 1996. *Victoria-150,* designed and built by Lindsay Cunningham, was the first C Class to effectively use a multi-slotted aerofoil wing section as a sail. Lindsay built several other yachts for the defence of the Little America's Cup and recognised the speed potential of the wing sail. This lead to the development of both *Yellow Pages Endeavour* and *Macquarie Innovation* as speed record yachts.

Timing of the record attempt by the Macquarie team employed a clever low-tech solution developed by the team in previous attempts and now embodied in the ISAF/WSSRC rules. It uses a video camera mounted in the crew pod and aimed to capture images of the transit posts onshore. The camera is capable of recording images at 25 frames per second. The transit posts, placed 8 metres apart in pairs, define start and finish lines of the 500-metre course. As the yacht passes the start line the video camera records an image of two starting posts in transit and some time later, crossing the finish line, records another image of the finish posts in transit.
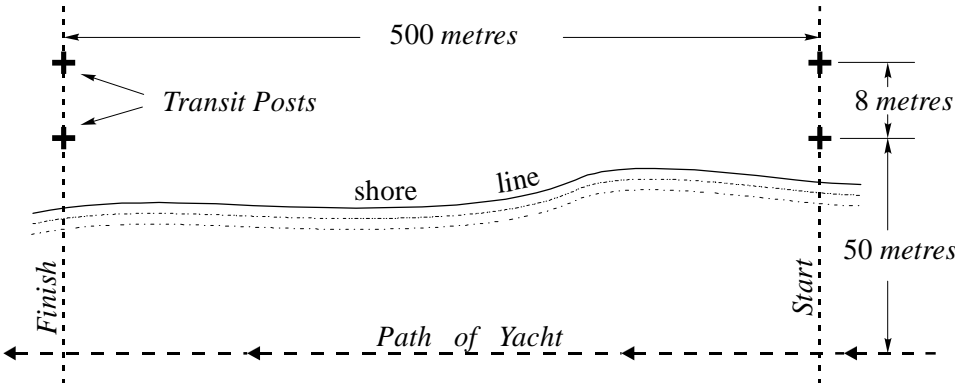
Figure 1. Schematic plan of transits posts defining the course

Video image frame *n*
just before crossing finish line

Video image frame *m*
just after crossing start line
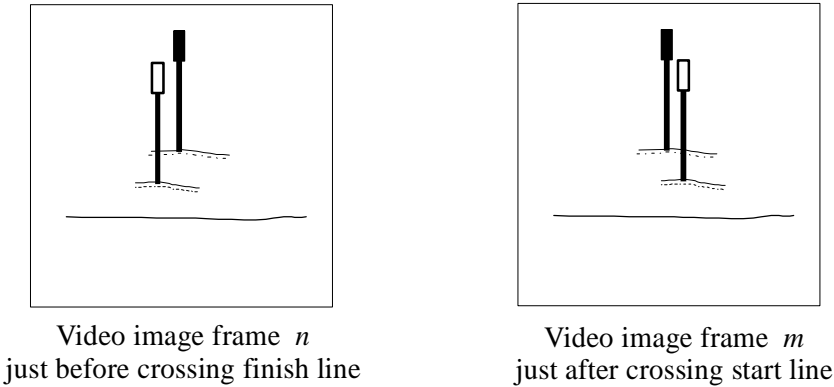
Figure 2. Diagrammatic view of the transit posts in video
image frames *m* and *n* at the start and finish lines.

After a run on the course, the video is reviewed frame by frame, noting the frame numbers *m* and *n* showing the start and finish transits(see Figure 2). Subtracting frame numbers and multiplying by the frame rate gives the elapsed time, which divided into the distance yields the average speed.

This timing technique, video camera and transit posts, presents some difficulties and restrictions for competing teams.

(1) The positioning of the transit posts is critical; not only must they produce parallel transit lines but these lines must be at least 500 metres apart and approximately perpendicular to the path of the yacht. This requirement necessitates a survey to mark the positions of the posts and a plan endorsed by a surveyor to satisfy the ISAF/WSSRC commissioner.
(2) The yacht is restricted to sailing close to the shore (and transit posts) so that video images of transits are clear and distinct.
(3) Since the yacht must travel relatively close to the transit posts and at great speed, there is some danger to the crew if the yacht became uncontrollable and collided with the transit posts.
(4) The direction of the shore (and hence the course) limits the allowable wind direction since a yacht's maximum potential speed is restricted to a narrow range of wind angles from the direction of travel.
(5) The video camera must be calibrated to ensure an accurate frame rate.
(6) Reviewing the video images is a time consuming process and is subject to human error (errors in visually interpreting the actual transit).

Recognising these restrictions, the Macquarie team approached the Department of Geospatial Science, RMIT, with a proposal to investigate the use of on-board GPS as a more flexible means of determining sailing velocity and distance. GPS has the following attractions and possible advantages over the present method.

(1) GPS is a proven robust positioning technology, well documented in the surveying and geodetic literature (Parkinson & Spilker 1996). When used in *kinematic differential* mode, GPS is capable of determining positions at centimetre level precision at precise and regular time intervals as small as 0.1 sec (Herbet *et al* 1997, and Ryan *et al* 1997).
(2) Kinematic Differential GPS positioning removes the restriction of marked courses. Positions can be determined at time intervals, say $\Delta t = 0.1 \sec$, independent of the yacht's sailing direction. Differences in position divided by time differences, yield velocity. In addition, simple velocity plots can be used to determine which section of a yacht's speed record attempt should be used to determine average velocity.

This paper presents an analysis of both methods (GPS and video) of determining sailing velocity. Simulations of GPS position recording and video recording were made during a recent record attempt by mounting a GPS receiver and the video camera on the Macquarie team's powerboat and making three runs along the marked course. Comparing the GPS-derived velocity with the video-derived velocity is a useful means of benchmarking GPS velocity against an approved ISAF/WSSRC technique. In addition, a Kalman filter is used to assess the precision of kinematic GPS positions and verify a simple method of determining approximations to instantaneous velocity from kinematic GPS.

This paper also provides an analysis of the survey made to position the timing transit posts at Shallow Inlet and the accuracy of sailing course distances defined by transit posts.

THE SHALLOW INLET COURSES

Shallow Inlet is a narrow curving body of water following the Bass Strait coastline of Waratah Bay near Wilsons Promontory, Victoria, Australia. The small coastal township of Sandy Point is situated nearby. The sailing courses on the inlet are located at a place where there is only a narrow strip of low sand dune separating the inlet from Bass Strait and the prevailing south-westerlies blow unimpeded across the courses. The beach is quite steep and the shore line curves in a south-east direction for approximately 2 kilometres. The steep beach means that relatively deep water close to shore is protected from the wind blowing off Bass Strait; smooth water for optimum sailing conditions.
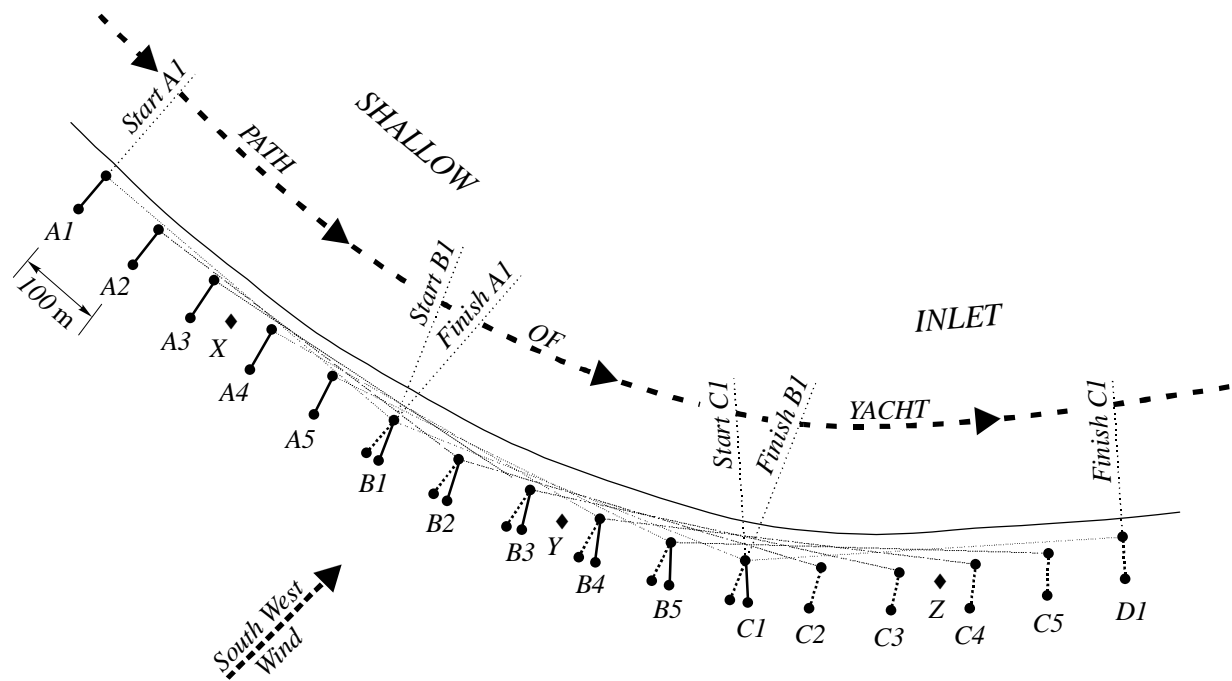
Figure 3. Schematic plan of sailing courses at Shallow Inlet showing the path of the yacht, front and rear transit posts (●) and survey control marks (♦)

Figure 3 shows a schematic diagram of the sailing courses at Shallow Inlet. Eleven (11) separate courses, each slightly in excess of 500 metres, were set out on the shoreline; designated *A1* to *A5, B1* to *B5* and *C1*. Each course has a pair of transit posts at the start and finish and individual courses were separated by approximately 100 metres. Each course is designated by its starting transit line; course *A1* starts at *A1* and finishes at *B1,* course *A2* starts at *A2* and finishes at *B2* etc. The last course *C1* starts at *C1* and finishes at *D1*. Hence, the *A-courses* start at *A*-marks and finish at *B*-marks, the *B-courses* start at *B*-marks and finish at *C*-marks and the single *C-course* starts at *C1* and finishes at *D1*. The middle group of courses have three transit posts at the start and finish, one in front and two at the rear. The front post and one of the rear posts defined a finish line of one course and the front post and the other rear post defined the start of another. The combined courses extended for approximately 1.5 km along the shoreline with courses having varying magnetic bearings, the first course *A1* 130° 25', the middle course *B1* 111° 36' and the last course *C1* having a bearing of 86° 27'.

Two surveys of the sailing courses were made; the initial set-out survey using a Leica TC805 Total Station and MC5 data collector and a subsequent survey using Trimble GPS equipment in *Rapid Static* differential mode. The second survey was used as a means of assessing the precision of the original survey.

COURSE DESIGN AND TOTAL STATION SURVEY

Three control marks (♦) *X, Y* and *Z* (see Figure 2) were established at approximately 500 metre intervals along the shore with mark *X* about 250 metres south-east of the start of course *A1*. A Total Station survey, using the data collector to record the measurements was performed connecting the control points *X, Y* and *Z* to the approximate locations of start and finish posts. Arbitrary coordinates of 2000.0 E and 3000.0 N were assigned to *Z* and the datum for bearings was magnetic north. The survey information was downloaded into LISCAD Surveying and Engineering Software (© Listech Pty Ltd) and the courses 'designed'. The course design process was as follows:

- Using the approximate start and finish locations of a particular course, the course bearing is computed.
- Fixing the coordinates of the start (front) transit post adopting the course bearing and a distance of 500.3 metres (more about this later), the coordinates of the finish (front) transit post are computed and stored.
- With the front start and finish transit posts fixed (and the bearing and distance between them known) the positions of the rear transit posts are fixed by perpendicular bearings and offset distances of 8 metres.
- With the position of transit posts computed and stored, the positions of reference points, 1 metre along transit lines were also computed and stored (see Figure 4). The reference points, 44 in total, were the points actually marked on the ground.

A Table of the designed Sailing Course bearings and distances is shown below. See Figure 3 for a schematic diagram of the courses.

Course	Bearing (Magnetic)	Distance (metres)
A1	130° 25'	500.27
A2	127° 18'	500.30
A3	123° 28'	500.30
A4	119° 46'	500.30
A5	116° 12'	500.30
B1	111° 36'	500.30
B2	106° 34'	500.30
B3	102° 25'	500.30
B4	096° 58'	500.30
B5	091° 41'	500.30
C1	086° 27'	500.30

Table 1. Sailing Course Bearings and Distances

After designing the courses, the coordinates of 38 transit posts, 44 reference points and the three control points *X, Y* and *Z* were uploaded into the data collector. The reference points (see Figure 3) for each start and end line were then marked in the field with 600 mm long, 50 mm square wooden pegs driven slightly below ground level.
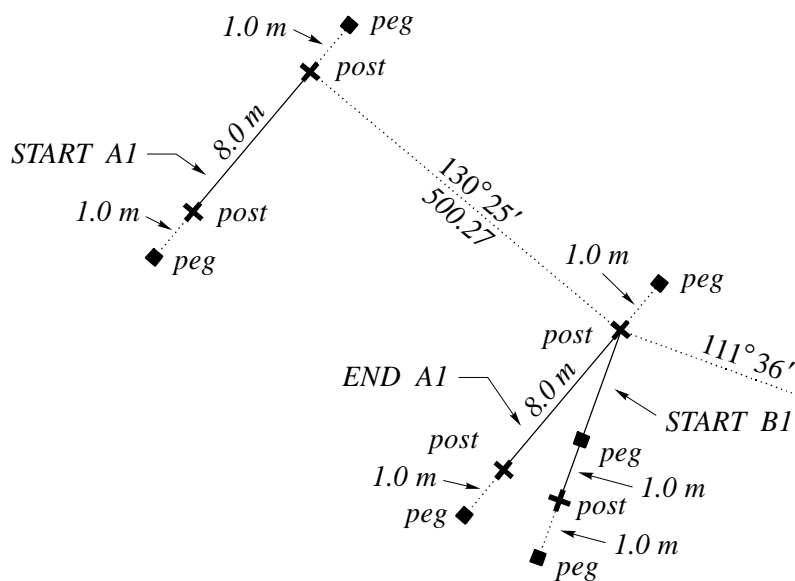
Figure 4. Schematic diagram of transit posts and reference pegs for
the start and end lines for Course *A1* and the start line of Course *B1*

After placing the reference pegs, members of the Macquarie team then positioned the transit posts using string lines and offset distances for position and a levelling staff bubble to ensure the posts were vertical.

ACCURACY OF THE COURSE DISTANCES

At Shallow Inlet, the high and low tidal range is approximately 1.5 metres. At high tide, the water's edge reaches the transit posts and at low tide, the water's edge is approximately 20-30 metres from the front transit posts. Attempts on the speed record are restricted to short periods of approximately one hour either side of high or low water thus ensuring that the tidal stream is below the allowable 1 knot under the ISAF/WRSSC rules. At high water, the yacht sails within 20-30 metres of the transit posts and at low water within 30-50 metres; 50 metres being the probable maximum distance between the yacht and the transit posts.

Marking the transit post reference pegs was done by radiation from the three control points *X, Y* and *Z* and no radiation distance exceeded 250 metres. It was estimated that the reference pegs could be placed within ±0.01 metres of their designed location; a reasonable assumption given the maker's specifications of the Leica TC805 Total Station, ±(0.003 + 2 ppm) for distances and ±3" for horizontal direction. (This estimated precision was confirmed by the Rapid Static GPS survey performed two weeks after the initial survey. Comparisons between the two surveys are detailed in a following section.)

Assuming no error in positioning the posts from the reference pegs and the posts being exactly 8 metres apart, the following assumptions can be used in a simple error analysis of the yacht's path distance. (i) maximum distance of 50 metres from the yacht's path to front transit posts and (ii) positional error of posts ±0.010 metres.

6
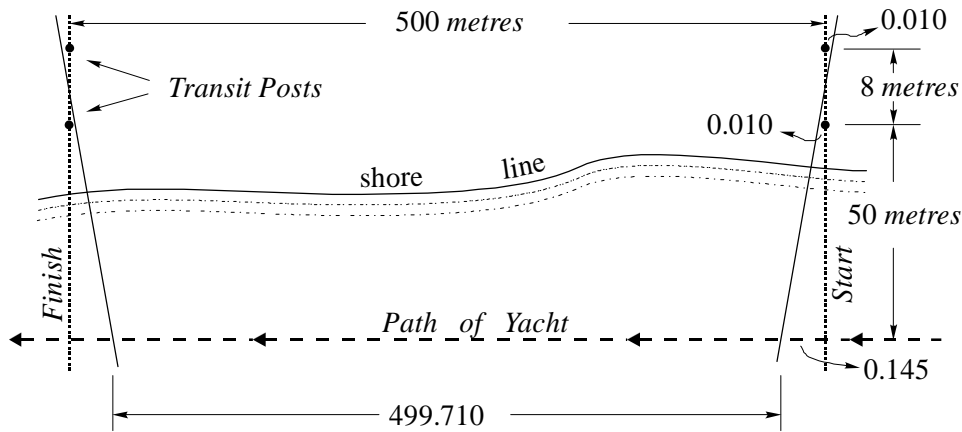
Figure 5. Error in transit lines and course length due to error in position of posts.

Referring to Figure 5 and using similar triangles to establish the ratios $\frac{x}{58} = \frac{0.020}{8}$ gives the error x at one end of 0.145 metres. If the error in both transit lines had the worst effect the yacht would only travel a distance of 499.710 metres. To allow for this possibility whilst ensuring that the yacht travelled at least 500 metres the course distance was adopted as 500.3 metres.

It is interesting to note that a yacht travelling at 48.60 knots has a velocity of 25.00 m/s knots (1 knot = 1 nautical mile per hour and by definition 1 nautical mile = 1852 metres exactly). A yacht travelling at this speed covers 500 metres in 20.00 seconds. The Macquarie team's video camera records at 25 frames per second and they use frame splitting to divide a single image into four parts; allowing the estimation of a transit to 1/100th of a second. This translates to a determination of the yacht's position along its path accurate to 0.25 metres if it's travelling at 48.6 knots, very close to the existing record.

GPS SURVEY OF REFERENCE MARKS

Two weeks after the initial survey and placement of the reference pegs a GPS survey of selected points was performed. Trimble 5700 geodetic receivers were used in *rapid static differential* mode with a base station set over the rear reference peg of the start line for course *A1*. GPS carrier phase data was collected at a rate of 5 measurements per second and each point was occupied for a minimum of 20 seconds. The reference pegs for all of the front transit posts were occupied as well as the reference pegs for the rear transit posts of the finish lines of courses *B2, B3, B4, B5* and *C1*. The control point *Z* was also occupied, making 22 points in total (not including the base station). The data was post-processed using Trimble Geomatics Office Version 1.5, ©Trimble Navigation Ltd. yielding 22 coordinate triplets (east, north and elevation) related to an arbitrary local coordinate system with values 0.000 E and 0.000 N at the base station. Inspection of the derived elevations indicated that the data for the front reference mark of the finish line for course *C1* was faulty and its coordinates were rejected, leaving 22 points (including the base station) for comparison.

Comparison between the two surveys, the initial Total Station survey and the rapid static GPS survey, was done by transforming the GPS coordinates to the coordinate system of the Total Station survey by using a 2D Linear Conformal transformation model of the form

$$E_k + v_E = a\,X_k - b\,Y_k - T_E$$
$$N_k + v_N = b\,X_k + a\,Y_k - T_N$$

(1)

E_k, N_k and X_k, Y_k are coordinates of the kth point in the Total Station survey and the GPS survey coordinate systems respectively, v_E, v_N are small unknown corrections (residuals) added to the left-hand side of equation (1) to allow for inconsistencies in the model caused by errors in the coordinates (the measurements), a, b are unknown coefficients and T_E, T_N are unknown translations. Each point yields two equations of the form (1) thus there will be 44 equations in the four unknown parameters a, b, T_E and T_N. The *least squares* principle was used to calculate the best estimates of the parameters, ie values of a, b, T_E and T_N that make the sum of the squares of the residuals a minimum. The scale factor s between measurements in both systems and the rotation θ between the coordinate axes is linked to the coefficients a and b

$$s = \sqrt{a^2 + b^2}$$
$$\theta = \tan^{-1}\left(\frac{b}{a}\right)$$

(2)

The computed parameters were $a = 0.975116$, $b = 0.221664$, $T_E = 898.508\,\mathrm{m}$ and $T_N = 3514.746\,\mathrm{m}$ giving the scale factor $s = 0.999993$ and rotation $\theta = 12°48'$.

The residuals v_E, v_N, computed from (1) and radial distances $r = \sqrt{v_E^2 + v_N^2}$ are shown Table 2 and can be used to assess the 'quality' of the surveys.

Reference point	v_E	v_N	r	Reference point	v_E	v_N	r
A1 (front, start)	0.000	0.005	0.005	B2 (front, finish)	-0.001	-0.008	0.008
A2 (front, start)	0.009	-0.005	0.010	B3 (front, finish)	-0.008	-0.004	0.009
A3 (front, start)	-0.004	0.003	0.005	B4 (front, finish)	0.003	0.006	0.007
A4 (front, start)	0.005	0.002	0.006	B5 (front, finish)	0.003	0.030	0.030
A5 (front, start)	0.006	0.047	0.047	C1 (rear, finish)	0.008	0.006	0.010
B1 (front, start)	0.015	-0.002	0.015	B5 (rear, finish)	-0.002	-0.014	0.014
B2 (front, start)	-0.005	-0.007	0.009	B4 (rear, finish)	0.006	0.004	0.007
B3 (front, start)	0.000	-0.006	0.006	B3 (rear, finish)	-0.009	0.004	0.010
B4 (front, start)	-0.013	-0.009	0.016	B2 (rear, finish)	0.001	0.005	0.006
B5 (front, start)	-0.010	-0.025	0.027	A1 (rear, start)	-0.006	-0.005	0.008
C1 (front, start)	-0.001	-0.010	0.010	Z (control point)	0.004	-0.007	0.008

Table 2. Transformation results, residuals v_E, v_N and radial distances $r = \sqrt{v_E^2 + v_N^2}$

If we consider the GPS survey as exact, the scale factor could be interpreted as a scale error of 7 parts per million in the Total Station distance measurements. The rotation is approximately equal to the magnetic variation; to be expected since the GPS local coordinate system has the north axis in the direction of the meridian through the base station. The sample mean and standard deviation of the 22 radial distances in Table 2 are $\bar{x} = 0.012$ metres and $s_x = 0.010$ metres respectively. These values are confirmation of the assumption that the reference pegs of the Total Station set out survey have a positional accuracy of ±0.010 metres.

SIMULATED SPEED RUNS USING KINEMATIC GPS AND VIDEO

On the same day as the GPS survey of the reference marks, speed trials with the Macquarie team's powerboat, were conducted on the Shallow Inlet course to compare velocities determinations by GPS and the Macquarie team's video camera. Three speed runs were made over the course; the GPS roving receiver and antenna mounted on the boat (with a base station on shore) and the team's video camera operating as it would if it were on board the yacht.

The following sections detail the GPS data acquired during the test, a method of deriving velocities from positions (East and North coordinates recorded at 0.1 second intervals) and comparisons with video derived velocities. Matlab, a software product of MathWorks™ was used to analyse the GPS data and produce the plots.

GPS Post-Processed Kinematic (PPK) data

GPS data were collected using Trimble 5700 receivers in kinematic differential mode recording carrier phase data at 0.1 second intervals. The base station was set over the rear reference peg of the start line for course *A1* (same as for the GPS survey of the reference marks) and the roving receiver and antenna were mounted on the team's powerboat. The observations were post processed (using Trimble Geomatics Office) yielding a data set containing 12,281 coordinate triplets (east, north and elevation) related to an arbitrary local arbitrary system with values of 0.000 E and 0.000 N at the base station. The coordinates were then transformed to the datum of the Total Station survey using the parameters determined previously creating a kinematic GPS data set having the following form

```
Sandy Point sailing simulations, PPK GPS survey, Feb 2002
All data
Epoch       Time        East        North       Distance
    0          0      898.508    3514.746         0.000
    1        0.1      925.502    3535.954        34.329
    2        0.2      925.505    3535.955        34.332
    3        0.3      925.502    3535.957        34.336
    4        0.4      925.505    3535.956        34.340
    5        0.5      925.500    3535.958        34.345
    .          .          .           .             .
    .          .          .           .             .
    .          .          .           .             .
12275     1227.5      931.026    3534.090      7965.918
12276     1227.6      931.023    3534.095      7965.923
12277     1227.7      931.022    3534.096      7965.924
12278     1227.8      931.019    3534.100      7965.930
12279     1227.9      931.018    3534.105      7965.935
12280     1228.0      931.019    3534.103      7965.937
```

Table 3. Extract from kinematic GPS data set.

The data for Epoch 0 relates to the GPS base station and subsequent data relate to positions determined at 0.1 second intervals. The Distance *s* is the along-track distance, ie the cumulative distance along the path of the receiver affixed to the powerboat and Time *t* is the time in seconds from the start of the survey.
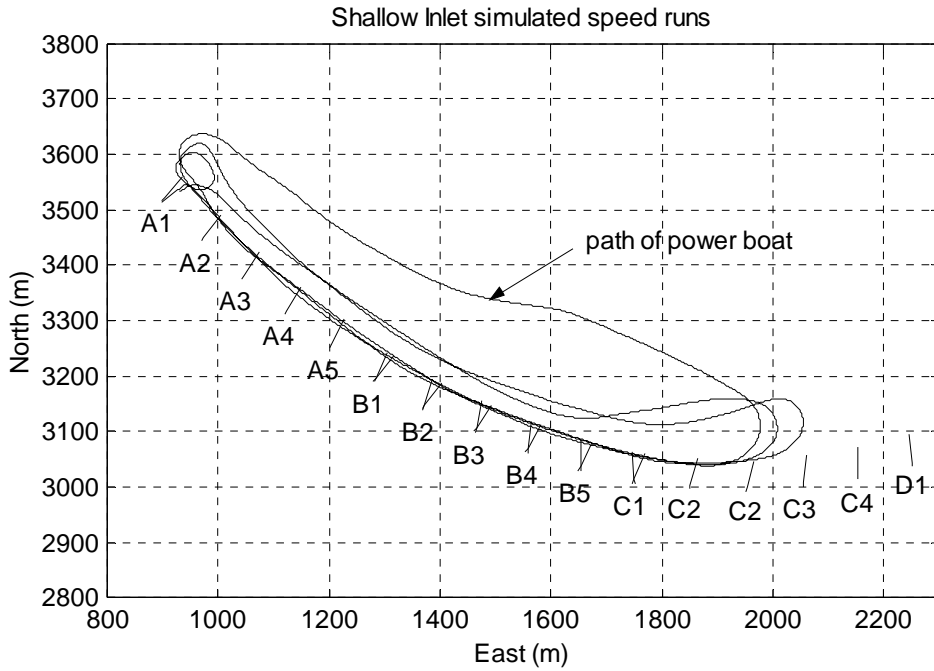
Figure 6. Path of powerboat on simulated speed runs at Shallow Inlet.

Figure 6 shows the path of the powerboat determined by the kinematic GPS survey recording carrier phase data at 0.1 second intervals. The start and finish transits (extended 50 metres from the front transit posts) of the eleven separate 500 metre courses are shown; *A1* to *A5*, *B1* to *B5* and *C1*. Course *A1* starts at *A1* and finishes at *B1*, course *A2* starts at *A2* and finishes at *B2* etc. The last of the eleven courses is *C1*, starting at *C1* and finishing at *D1*.

The powerboat made three separate runs along the shoreline. Each run started near *A1* with the powerboat accelerating to a maximum velocity near *A4*, maintaining this speed until passing *C1*, the finish transit for course *B1* and then returning to *A1*.

Velocity derived from kinematic GPS positions using approximations to calculus

Kinematic GPS positions (East and North coordinates at instants of time t_k) can be used to derive approximations to instantaneous velocity V by dividing the distance travelled from t_k to t_{k+1} by the time interval $\Delta t = t_{k+1} - t_k$. If the velocity is constant (or nearly so) and the GPS positions are exact then this simple approximation would be sufficient. In practice, the velocity is not generally constant and the GPS coordinates have small positional errors; these factors can lead to relatively large fluctuations in derived velocities if Δt is small. The following section outlines the derivation of a more realistic estimate of V using Taylor's theorem and an assumption that the distance travelled

increases according to the familiar equation from dynamics; $s_k = s_{k-1} + V_{k-1}\Delta t + \frac{1}{2}a\,\Delta t^2$ (s_k is the

distance travelled at time t_k and a is acceleration). The Law of Propagation of Variances is then applied to this formula to derive a suitable time interval Δt taking account of the positional accuracy of the GPS coordinates.

10

Kinematic GPS positions at instants of time t_k can also be converted to cumulative distances s_k measured along the path of the receiver from the start of the survey where $t_0 = 0.0$ seconds and $s_0 = 0.000$ metres . The distance s can be considered as a continuous function of t, written as $s(t)$ with velocity V as the first derivative $s'(t)$

$$V = s'(t) = \lim_{\Delta t \to 0} \frac{s(t + \Delta t) - s(t)}{\Delta t} \tag{3}$$

Using the distances s_k at times t_k, which can be regarded as discrete measurements of the continuous function, an approximation of the velocity can be developed by considering the following.

The function $s(t)$ can be expanded using Taylor's theorem

$$s(t) = s(t_k) + (t - t_k)s'(t_k) + \frac{(t - t_k)^2}{2!} s''(t_k) + \frac{(t - t_k)^3}{3!} s'''(t_k) + \mathrm{L} + \frac{(t - t_k)^{n-1}}{(n-1)!} s^{(n-1)}(t_k) + R_n$$

where $s(t_k)$ is the function evaluated at time t_k, $s'(t_k)$ is the derivative evaluated at t_k with higher order derivatives written as $s''(t_k)$, $s'''(t_k)$, L , etc and R_n is a remainder. Letting $t = t_k + \Delta t$ gives another form of Taylor's theorem

$$s(t_k + \Delta t) = s(t_k) + \Delta t \, s'(t_k) + \frac{\Delta t^2}{2!} s''(t_k) + \frac{\Delta t^3}{3!} s'''(t_k) + \mathrm{L} \tag{4}$$

Replacing Δt with $-\Delta t$ gives

$$s(t_k - \Delta t) = s(t_k) - \Delta t \, s'(t_k) + \frac{\Delta t^2}{2!} s''(t_k) - \frac{\Delta t^3}{3!} s'''(t_k) + \mathrm{L} \tag{5}$$

and subtracting (5) from (4) gives

$$s(t_k + \Delta t) - s(t_k - \Delta t) = 2\Delta t \, s'(t_k) - 2\frac{\Delta t^3}{3!} s'''(t_k) - \mathrm{L} \tag{6}$$

If the yacht is moving along the course in a relatively straight line then, over a short time interval, its position at t_k is approximated by $s(t_k) = s(t_{k-1}) + s'(t_{k-1})\Delta t + \frac{1}{2}s''(t_{k-1})\Delta t^2$ the familiar equation from dynamics and the 3rd derivative $s'''(t_k) = 0$ as will all other higher order derivatives, hence (6) can be re-arranged as

$$V = s'(t_k) = \frac{s(t_k + \Delta t) - s(t_k - \Delta t)}{2\Delta t} \tag{7}$$

Equation (7) is the first order central difference approximation of the velocity V (Dahlquist and Björck 1974, Bruton *et al* 1999, and Ryan *et al* 1997).

Velocities determined using (7) have a precision that is a function of the precision of the distances s at times $t_k \pm \Delta t$. The times t_k and t_{k-1} can be considered as exact since the receiver time of observation is synchronised with atomic clocks on board the GPS satellites. These GPS atomic clocks, used to generate the carrier waves for the broadcast message, are accurate to $\pm 10^{-13}$ seconds. For the kinematic survey, the GPS coordinates are assumed to have a precision of $\sigma_E = \sigma_N = 0.010$ metres . These values are consistent with the positional accuracy deduced from the comparison of the Total Station and Rapid Static surveys of the reference marks. σ_E and σ_N can be transformed to a distance

precision $\sigma_s = \sqrt{\sigma_E^2 + \sigma_N^2}$ that can be used to assess the precision of computed velocities by using the Law of Propagation of Variances with the distances considered as independent random variables.

Consider three distances s_1, s_2 and s_3 at equally spaced intervals of time t_1, t_2 and t_3 where $\Delta t = t_3 - t_2 = t_2 - t_1$, then by (7) the velocity at t_2 is $V = \dfrac{s_3 - s_1}{2\Delta t}$. The variance of V is given by

$$\sigma_V^2 = \left(\frac{\partial V}{\partial s_3}\right)^2 \sigma_{s_3}^2 + \left(\frac{\partial V}{\partial s_1}\right)^2 \sigma_{s_1}^2 \tag{8}$$

with derivatives $\dfrac{\partial V}{\partial s_3} = \dfrac{1}{2\Delta t}$ and $\dfrac{\partial V}{\partial s_1} = \dfrac{-1}{2\Delta t}$ and precisions $\sigma_{s_3}^2 = \sigma_{s_1}^2 = \sigma_s^2$. Substituting into (8), re-arranging and taking square roots gives the standard deviation (precision) of the computed velocity

$$\sigma_V = \frac{\sigma_s}{\sqrt{2}\,\Delta t} \tag{9}$$

Equation (9) can be used to determine an appropriate time interval Δt given σ_s and a desired σ_V, for example, if it is desired to estimate the velocity with a precision of $\sigma_V = 0.05$ knots and the precision of the distances is $\sigma_s = 0.015$ metres then

$$\Delta t = \frac{\sigma_s}{\sqrt{2}\,\sigma_V} \times \frac{3600}{1852} = 0.4\,\mathrm{sec}$$

Using equation (7) with $\Delta t = 0.4\,\mathrm{sec}$ Velocities V_n (knots) and times t_n (seconds) were computed from the kinematic GPS data set. Figure 6 shows a schematic diagram of the data set with $k = 12{,}280$ distances s_k at 0.1 second intervals (epoch 1 to epoch 12280). With $\Delta t = 0.4\,\mathrm{sec}$ (4 epochs) there will be $n = k - 8 = 12{,}272$ derived velocities. The first velocity $V_1 = \dfrac{s_9 - s_1}{0.8}$ at time $t_1 = 0.5\,\mathrm{seconds}$, the second velocity $V_2 = \dfrac{s_{10} - s_2}{0.8}$ at $t_1 = 0.6\,\mathrm{seconds}$ and so on. The last velocity $V_n = \dfrac{s_k - s_{k-8}}{0.8}$ at $t_n = t_{k-4} = 1227.6\,\mathrm{seconds}$.
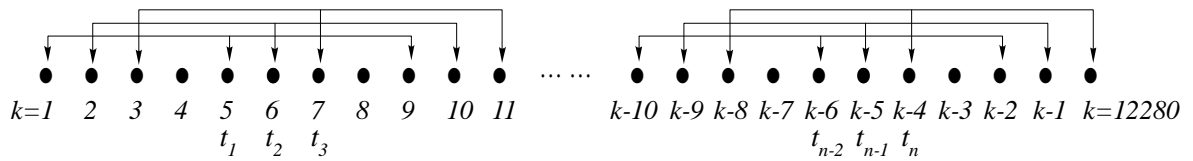
Figure 7. Schematic diagram of the distances s in the kinematic GPS data set.

Figure 8 shows a plot of the derived velocities V_n (knots) with the three runs along the course distinguished by their higher average velocity. At the start of the kinematic GPS survey, the powerboat was stationary during a receiver initialisation period of approximately 8 minutes.
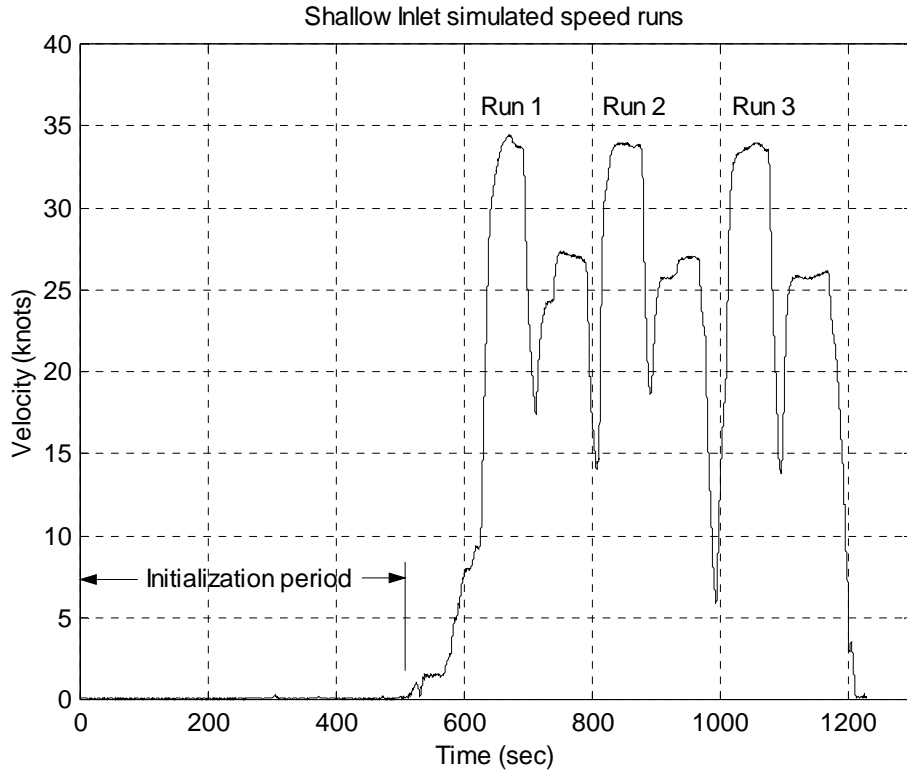
Figure 8. Velocity plot of simulated speed runs at Shallow Inlet

GPS transit epochs

In Figure 6 the path of the powerboat's three runs over the course is shown with the transit lines extended 50 metres from the front transit post. Figure 9 shows an enlargement of the powerboat's path on Run 2 near the starting transit line for course A5. Epoch numbers are shown beside individual points (East and North coordinates). By inspecting such enlargements, it was possible to determine the epochs when the powerboat was <u>on or near</u> transits. These are shown in Table 4 with the relevant extracts from the kinematic GPS data set shown in Table 5.
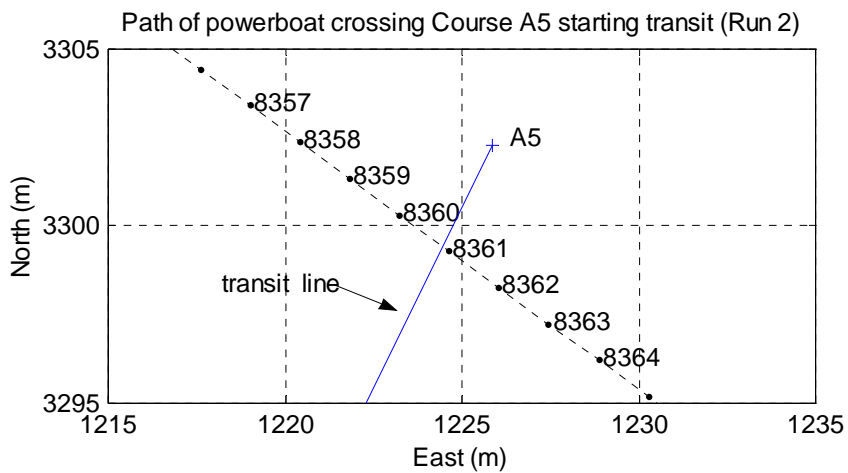
Figure 9. Path of powerboat in the vicinity of starting transit for Course *A5,* Run 2

Course	Epoch (start)	Epoch (finish)
A1	8107	8426
A2	8186	8482
A3	8248	8538
A4	8305	8594
A5	8361	8650
B1	8416	8706
B2	8471	8762

Table 4. Start and finish epochs for Courses *A1* to *A5, B1* and *B2*, Run 2

```
Epoch   Seconds      East       North      Distance
8107     810.7     942.641    3567.067    2772.359
8186     818.6     999.104    3484.341    2872.768
8248     824.8    1068.940    3414.124    2972.420
8305     830.5    1146.960    3357.682    3068.717
8361     836.1    1224.640    3299.254    3165.921
8416     841.6    1303.900    3245.375    3261.776
8426     842.6    1318.574    3235.929    3279.227
8471     847.1    1384.563    3193.207    3357.840
8482     848.2    1400.979    3183.271    3377.029
8538     853.8    1488.838    3140.675    3474.727
8594     859.4    1579.065    3103.698    3572.253
8650     865.0    1672.155    3075.807    3669.467
8706     870.6    1767.174    3054.705    3766.818
8762     876.2    1863.491    3041.643    3864.115
```

Table 5. Extract from the kinematic GPS data set.

Kinematic GPS velocity plots and the World Sailing Speed Record Council rules

The International Sailing Federation World Sailing Speed Record Council (ISAF/WSSRC) has established rules for World Records and sections 3 to 6 of the RECORD RULES 1999-2001 (WSSRC 2002) are reproduced below.

3. THE COURSE
The record shall be established over a minimum of half a kilometre on water (not ice).

The course may be defined by posts and transits ashore, or by buoys afloat.
Transits shall not converge.

4. TIMING
A timed run is measured from the difference in the times recorded at the crossing of the starting and finishing lines.

Where the timing positions are able to be land based, videoing, which includes a time display of the transits shall be used. Where timing positions are not land based, requests for an attempt without video must be made prior to the event.

In order to facilitate recognition, craft must carry clear and visible sail numbers to the satisfaction of the timing Commissioner on duty.

5. CALCULATION OF SPEED
Time shall be recorded to the nearest one hundredth of a second.
The speed shall be calculated to the nearest 1/100th of a knot with allowance made for the resolved component of any tidal stream and/or current on the course. A venue is not suitable for record breaking if the current is more than one knot. The stream or current shall be measured by float tests or other means as appropriate and the results supplied to the Official Commissioner (see Rule 14).

6. MARGINS
In order to establish a new record the new elapsed time (corrected to 500 metres precisely) must improve on the existing record by a margin as follows:

a. On a course using land based transits and video recorded timing.
Between records claimed on the same course and when the timing positions have not been moved, the margin is equal to the accuracy of the video equipment ie, on equipment recording to 1/00th second, the margin is 1/100th second, on equipment recording to 1/50th second, the margin is 1/50th second.

b. Between records claimed on different courses or when timing positions have been changed, the margin is to be 1/25th second.

c. When transits are afloat and/or no video is used, the margin shall be 1%.

The ISAF/WSSRC rules are essentially time-based and speeds (or velocities) are averages, calculated by dividing the course distance by the elapsed time. Kinematic GPS measurements provide accurate point positions (or cumulative distances) at regular and precise time intervals, in our tests, 1/10th of a second. Kinematic GPS cannot provide transit times to any better than 1/10th of a second but can provide:

(i)   average velocity derived from continuous estimates of a craft's velocity between times (epochs) which we shall call *Average 1* denoted as $A_1(V)$, or

(ii)   average velocity calculated from a distance between times (epochs) which we shall call *Average 2* and denote as $A_2(V)$ from which a time, corrected to 500 metres precisely, can be computed as per ISAF/WSSRC RECORD RULES – Section 6.

Figures 10 and 11 are plots of the powerboat's velocity on Run 2 along the course at Shallow Inlet with arrows indicating when it was passing the start and finish transit lines of various courses.
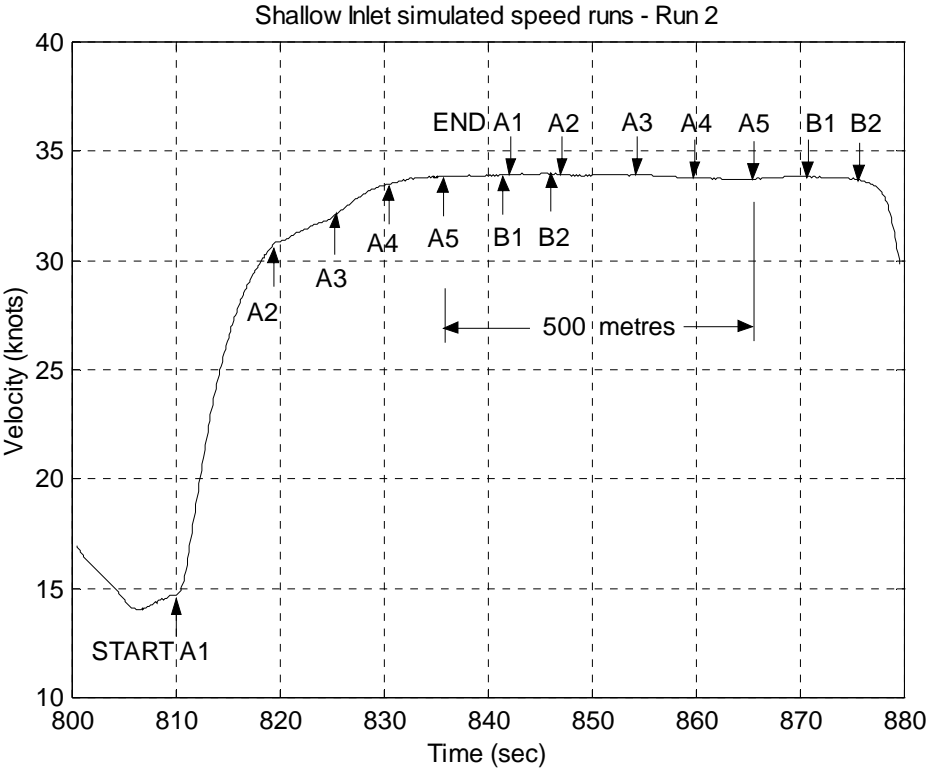
Figure 10. Velocity plot of Run 2 – Courses *A1* to *A5, B1* and *B2*

In Figure 10, arrows indicate start and finish transit times for courses *A1* to *A5, B1* and *B2*. Arrows on the lower side of the line indicate starts and on the upper side, indicate finishes. From the plot, the powerboat is accelerating from the start of course *A1* to the start of course *A4,* reaching a constant velocity of approximately 33-34 knots in the vicinity of the start of course *A5*. It maintains this velocity until reaching the end of course *B2*.

From a plot such as this, an average velocity could be obtained by drawing a straight line (parallel to the Time axis) and passing as nearly as possible through the plotted velocity curve, then interpolating the Velocity scale. This would only be practical when the craft had reached a nearly constant velocity eg, between the start of course *A5* and the end of course *B2*. At the scale of this plot, it would only be possible to estimate the average velocity to ±1-2 knots; well outside the margins specified in ISAF/WSSRC rules for a new record. To achieve a better resolution of velocity, enlargements of sections of the craft's path might be a solution, but this presents some problems as demonstrated in Figure 11.
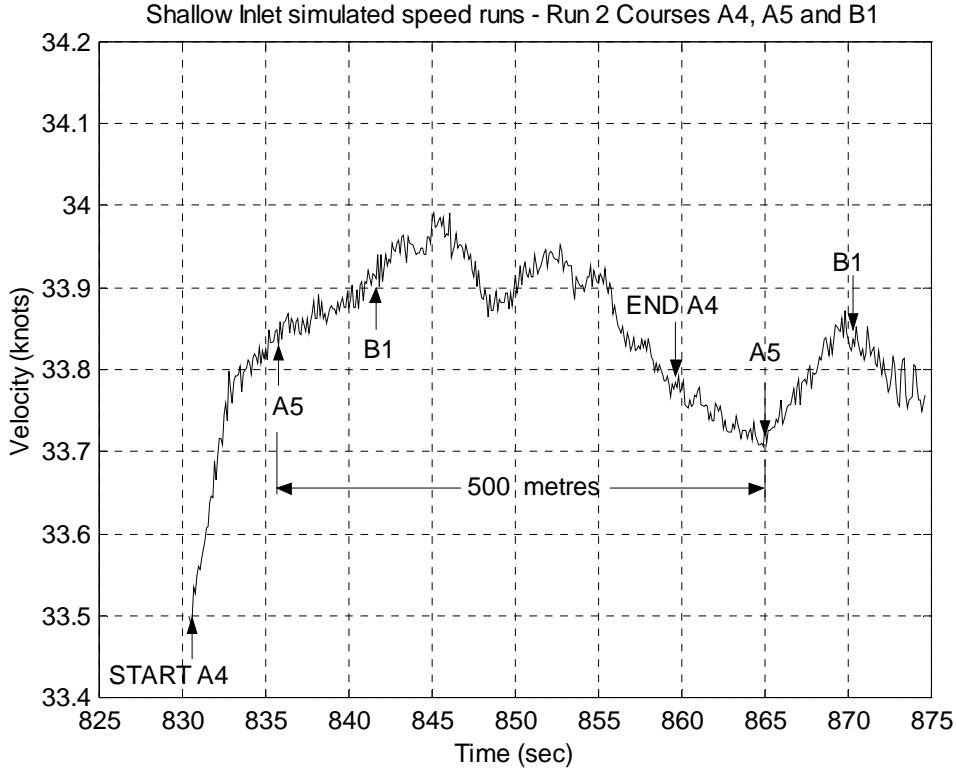
Figure 11. Velocity plot of part of Run 2 – Courses *A4, A5* and *B1*

In Figure 11, arrows indicate start and finish transit times for courses *A5, A5* and *B1;* again arrows on the lower side of the line indicate starts and on the upper side, indicate finishes. This plot is an enlargement of Figure 10 and shows a large variation of velocity (approximately 0.3 knots) between the start of course *A4* and the end of course *B1* and small fluctuations of ±0.05 knots of the velocity curve. Drawing lines to estimate average velocity on a graph such as this would be problematic at best.

These difficulties may be overcome if a graph was used to determine approximate starting and finish times and mathematics used to determine an average velocity based on the *mean value theorem* of integral calculus.

Average velocity $A_1(V)$ from kinematic GPS velocities

Velocities V_n derived from the kinematic GPS survey are discrete estimates of a continuous function that varies with time, ie $V = f(t)$. The mean value theorem of integral calculus (Apostol 1967) can be used to give $A_1(V)$, the average vale of *V* between times t_1 and t_n

$$A_1(V) = \frac{1}{t_n - t_1}\int_{t_1}^{t_n} V(t)\,dt \qquad (10)$$
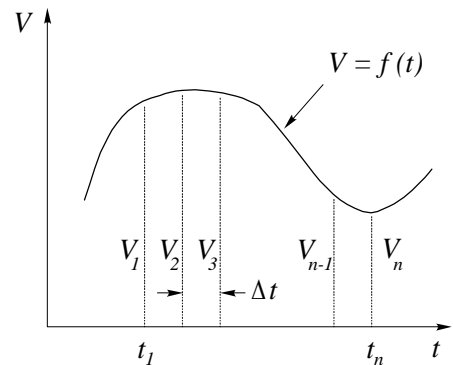
Figure 12

Referring to Figure 12, $A_1(V)$ the average value of the *V* between times t_1 and t_n, is the area under the curve (between t_1 and t_n) divided by the difference between t_1 and t_n. If values of the function are

known at discrete intervals Δt then the area under the curve may be approximated by the sum of the areas of a series of trapezoids and the average velocity is

$$A_1(V) ; \quad \frac{\Delta t}{t_n - t_1} \left(\frac{V_1 + V_n}{2} + V_2 + V_3 + \text{L} + V_{n-2} + V_{n-1} \right) \tag{11}$$

Average velocity $A_2(V)$ and corrected time T_C from kinematic GPS positions

Kinematic GPS provides East and North coordinates at regular and precise times. An average velocity $A_2(V)$, in knots, between start and finish times and time T_C, corrected (or adjusted) to a distance of exactly 500 metres, can be calculated from

$$chord\ dist = \sqrt{(E_{FINISH} - E_{START})^2 + (N_{FINISH} - N_{START})^2}$$
$$time = t_{FINISH} - t_{START}$$
$$A_2(V) = \frac{chord\ dist}{time} \times \frac{3600}{1852} \tag{12}$$
$$T_C = \frac{time \times 500}{chord\ dist}$$

In equations (12) the coordinates are in metres and the *chord distance* is the straight-line distance between coordinate distances at the start and finish times. The average velocity is in knots and the ratio 3600/1852 is a conversion factor from m/s to knots. In the case of a course marked by transit posts, the chord distance is the distance between transits. A yacht travelling along a path following a curving shoreline, as at Shallow Inlet, may travel a longer path distance. Velocities and corrected times calculated by (12) accord with the ISAF/WSSRC rules.

Table 6 shows average velocities $A_1(V)$, $A_2(V)$ and corrected times T_C for courses *A1* to *A5, B1* and *B2* on Run 2.

Course	Epoch (start)	Epoch (finish)	Chord Distance (metres)	Elapsed Time (sec)	$A_1(V)$ (knots)	$A_2(V)$ (knots)	T_C (sec)
A1	8107	8426	500.98	31.9	31.11	30.53	31.84
A2	8186	8482	502.14	29.6	33.16	32.98	29.47
A3	8248	8538	501.09	29.0	33.70	33.59	28.94
A4	8305	8594	501.22	28.9	33.87	33.71	28.83
A5	8361	8650	500.20	28.9	33.87	33.64	28.89
B1	8416	8706	500.98	29.0	33.85	33.58	28.94
B2	8471	8762	502.34	29.1	33.81	33.56	28.96

Table 6. GPS derived average velocities and corrected times Run 2 at Shallow Inlet

Note that over each of the five courses $A_1(V)$ is greater than $A_2(V)$. This is a reflection of the fact that the powerboat is travelling along a slightly curved path following the shoreline, covering a longer distance than the chord distance between the GPS positions at the starting and finishing epochs.

Differences in the average velocities over particular courses shown in Table 6 are significant. Excepting the first course *A1,* where the powerboat was still accelerating after crossing the starting transit, the average difference is 0.2 knots. A world record attempt on a curving course, such as Shallow Inlet, might fail simply because of the method of calculating velocities as stipulated in the ISAF/WSSRC rules. Theses rules make no allowance for the actual distance travelled

Average velocity $A_2(V)$ **and corrected time** T_C **from Video Camera**

During the simulated three speed runs in the powerboat, the Macquarie team's video camera was recording images of start and finish transits. Inspection of the video gave the following transit times on Run 2 shown in Table 7, together with the chord distances (as per the Table 1) and average velocity and corrected time computed using equations (12).

Course	Video (start)	Video (finish)	Chord Distance (metres)	Elapsed Time (sec)	$A_2(V)$ (knots)	T_C (sec)
A3	9m 10.64s	9m 45.16s	500.30	28.92	33.62	28.90
A4	9m 16.36s	9m 45.16s	500.30	28.80	33.77	28.78
A5	9m 21.92s	9m 50.84s	500.30	28.92	33.63	28.90
B1	9m 28.40s	9m 56.44s	500.30	28.04	34.68	28.02
B2	9m 33.96s	10m 01.96s	500.30	28.00	34.73	27.98

Table 7. Video Camera derived average velocities and corrected times Run 2 at Shallow Inlet

Comparing the average velocities $A_2(V)$ derived from GPS observations (Table 6) with those derived from Video Camera observations (Table 7) shows that GPS is a viable alternative to the video camera technique. The average difference for courses *A3, A4* and *A5* is 0.03 knots. The average difference for courses *B1* and *B2* is 1.13 knots which is significantly different from the first three courses. We suspect that this is due to human error in interpretation of the video images of the transits.

COMPARING VELOCITY (FROM CALCULUS) WITH VELOCITY FROM A KALMAN FILTER

A Kalman filter is a set of mathematical equations that are applied recursively to estimate the *state* of a dynamic system. In our case, the dynamic system is the powerboat (with GPS receiver) moving along the course. It receives position at time t_{k-1}, East and North (*E,N*) coordinates from kinematic GPS measurements (the *primary* measurement model), and moves to position t_k, according to a *dynamic* model, where it receives new position information. The state of the system at t_k is its position E_k, N_k, its velocity $\dot{E}_k, \dot{N}_k$ and acceleration $\ddot{E}_k, \ddot{N}_k$. A Kalman filter takes into account the precisions of the measurements and the dynamic model and provides an efficient (recursive) computational solution to a least squares estimate of the state. That is, if the true value of the measurements are the observed values plus small unknown corrections (residuals) and the dynamic model has residuals accounting for the difference between theory and practice, then a least squares solution provides estimates that make the sum of the squares of the weighted residuals a minimum value. The weight of an observation is a measure of its precision.

In 1960, R.E. Kalman published his famous paper describing a new approach to the solution of linear filtering and prediction (Kalman 1960) and since that time, papers on the technique have been filling numerous scientific journals. The Kalman filter is regarded as one of the most important algorithmic techniques ever devised and has been used in applications ranging from navigating the Apollo spacecraft to predicting short-term fluctuations in the stock market. Sorenson (1970) shows Kalman's technique to be an extension of Gauss' original method of least squares providing historical commentary on its connection with earlier work by 20th century mathematicians and (failed) claims to priority by his contemporaries. The derivation of the Kalman filter equations can be found in many texts eg. Brown and Hwang (1992), and Zarchan and Musoff (2000) have numerous examples of applications. A Kalman filter is relatively simple to implement on modern computers (a reason for its

popularity) and lends itself to practical applications such as the estimation of position, velocity and acceleration from kinematic GPS observations. Appendix A contains a summary of the necessary elements of a Kalman filter, a statement of the equations and a step by step outline of the recursive method of estimation of position, velocity and acceleration used in this paper.

The kinematic GPS data for Run 2 (epochs 8000 to 8800) was processed using a Kalman filter and plots of the filtered and unfiltered velocities are shown in Figures 13 and 14. Plots of corrections to the kinematic GPS coordinates and histograms of corrections are shown in Figure 15. In the Kalman filter we used a precision of kinematic GPS coordinates E_k, N_k of ± 0.010 metres and used a dynamic model linking the state (position, velocity and acceleration) at times t_{k-1} and t_k of

$$E_k = E_{k-1} + \dot{E}_{k-1}\Delta t + \tfrac{1}{2}\ddot{E}_{k-1}\Delta t^2$$

$$N_k = N_{k-1} + \dot{N}_{k-1}\Delta t + \tfrac{1}{2}\ddot{N}_{k-1}\Delta t^2$$

$$\dot{E}_k = \dot{E}_{k-1} + \ddot{E}_{k-1}\Delta t$$

$$\dot{N}_k = \dot{N}_{k-1} + \ddot{N}_{k-1}\Delta t$$

$$\ddot{E}_k = \ddot{E}_{k-1}$$

$$\ddot{N}_k = \ddot{N}_{k-1}$$

where $\Delta t = t_k - t_{k-1} = 0.1\,\text{sec}$. The dynamic model and the true relationship between successive states are assumed to differ by errors induced by small random changes in acceleration known as *jerk*. In our implementation, the precision of jerk was estimated to be ± 0.01 m/s^3.
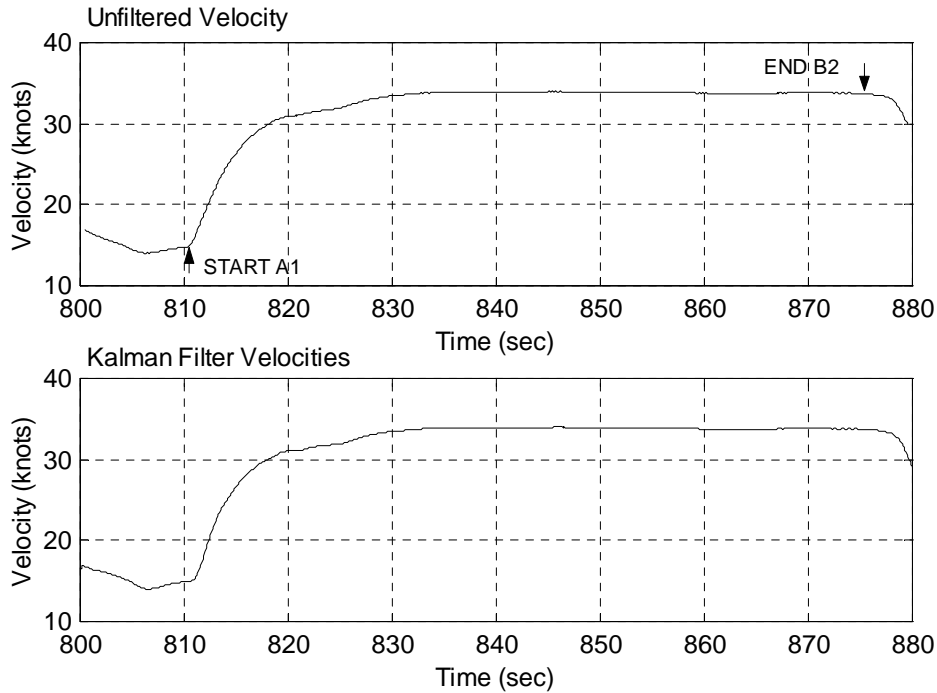
Figure 13. Unfiltered and filtered velocity plots of Run 2 – Courses *A1* to *A5, B1* and *B2*

In Figure 13, the unfiltered velocities are those obtained using equation (7) with $\Delta t = 0.4\,\text{sec}$ and shown in Figures 10 and 11. The filtered velocities are those obtained from the Kalman filter.

At the scale of the plots in Figure 13 there appears to be no discernible difference between the two velocity curves but an enlargement, Figure 14, shows the filtered velocities as a much smoother curve than the unfiltered velocities.
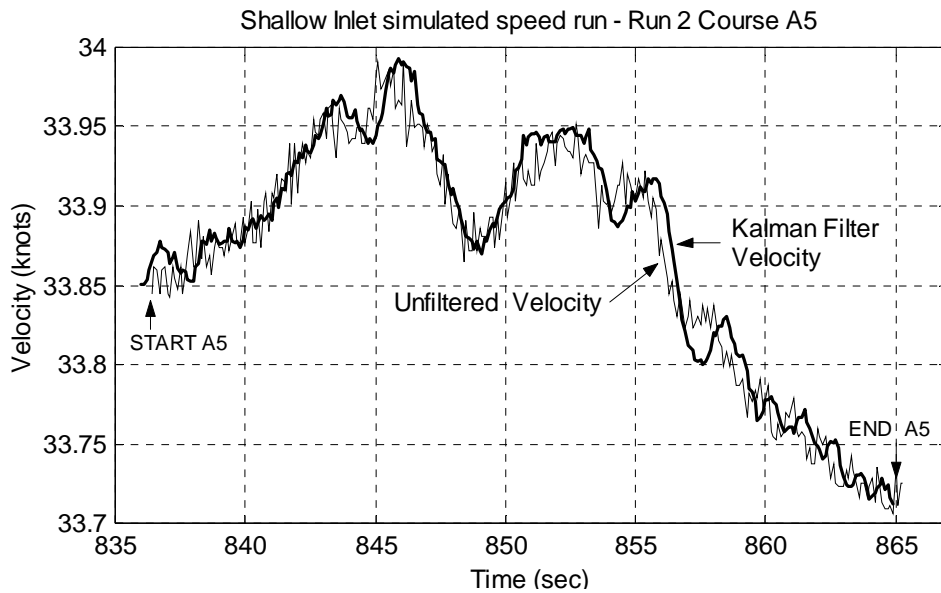
Figure 14. Unfiltered and filtered velocity plots of Run 2, Course *A5*

In Figure 14, the filtered velocity is generally close to the unfiltered velocity. Where acceleration is constant; from the start to 845 seconds, and 860 seconds to the end, the differences between the two curves are small, in the order of ±0.02 knots. Where acceleration is changing, the two curves depart. This is due to the precision of jerk in the Kalman filter. If this value is small, then the filtered velocity will be smooth but the dynamic model will be resistant to change causing the filtered velocity curve to lag the unfiltered curve where acceleration changes. If the precision of jerk is large, the dynamic model is more variable but the filtered velocity curve will have a more jagged appearance.

Choosing a suitable value for the precision of jerk requires some knowledge of the type of craft and its usual behaviour. For example, a Kalman filter used to model the movement of an oil tanker, would have a dynamic model with very small values of jerk, since its actual path and velocity would be highly resistant to small accelerations caused by wind, tide, changes in velocity etc. On the other hand, if we were modelling the movement of a small powerboat our dynamic model would have larger values of jerk, since its actual path and velocity would be more susceptible to accelerations.

In our implementation of the Kalman filter, the precision of jerk was estimated to be ±0.01 m/s^3. Is this a "good" value? Figure 15 shows plots and histograms of corrections to the kinematic GPS coordinates from the Kalman filter for Run 2. In general, the corrections are relatively small having a range of approximately 0.1 metres. For Course *A5,* where the powerboat has a relatively constant velocity, the corrections are very much smaller, having a range of approximately 0.03 metres; this would indicate that our value for the precision of jerk was reasonable. The large fluctuations in corrections are for the period of Run 2 where the powerboat is accelerating at the beginning of the run.
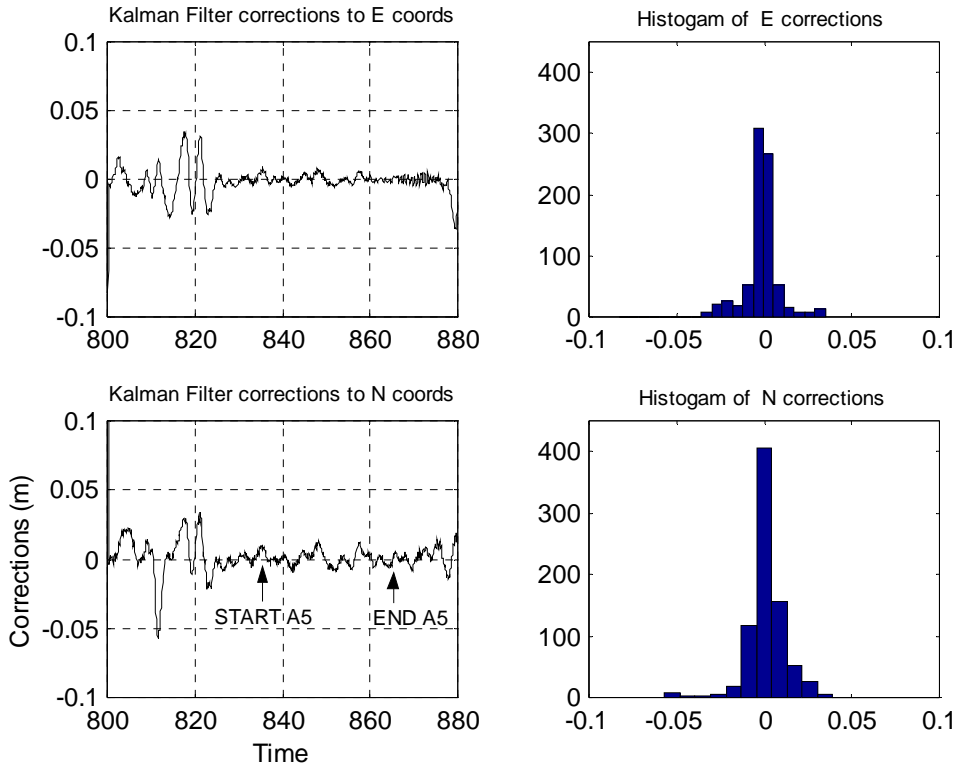
Figure 15. Kalman filter corrections to kinematic GPS coordinates
Run 2 – Courses *A1* to *A5, B1* and *B2*

A Kalman filter gives precision estimates of the state at every measurement update. At the end of the process, these estimates have been influenced by every measurement used. In our case epochs 8000 to 8800 were processed (800 measurements at 0.1 second intervals) and the state cofactor matrix $\mathbf{Q}_x$ for the last epoch is shown in Table 8. The filtered state vector is shown in the left column, the next column contains the corrections to the approximate values of the state vector. The block of numbers on the right are the elements of the 6 by 6 state cofactor matrix $\mathbf{Q}_x$; the diagonal elements are estimates of the variances of the elements of the state vector at epoch 8800 (the last measurement).

```
Epoch = 8800
Filtered State   Corrns    Filtered State cofactor matrix Q
                                                          x
 E 1926.482      -0.019    0.000035  0.000000  0.000075  0.000000  0.000081  0.000000
 N 3043.463       0.016    0.000000  0.000035  0.000000  0.000075  0.000000  0.000081
 Ve   14.852     -0.040    0.000075  0.000000  0.000261  0.000000  0.000388  0.000000
 Vn    1.779      0.033    0.000000  0.000075  0.000000  0.000261  0.000000  0.000388
 aE   -1.261     -0.043    0.000081  0.000000  0.000388  0.000000  0.000832  0.000000
 aN    0.823      0.036    0.000000  0.000081  0.000000  0.000388  0.000000  0.000832
```

Table 8. Kalman filter state vector, corrections and state cofactor matrix for epoch 8000.

From Table 8, the following estimates of the precision of the state are:

standard deviation of *E* and *N* coordinates: $\sqrt{0.000035} = 0.006$ m

standard deviation of *E* and *N* velocities: $\sqrt{0.000261} = 0.016$ m/s

standard deviation of *E* and *N* accelerations: $\sqrt{0.000832} = 0.029$ m/s^2

These estimates are influenced by the original assumptions of precision; position ±0.010 m and jerk ±0.01 m/s^3 but can be regarded as confirmation of the precision of the kinematic GPS coordinates.

In the preceding sections, unfiltered kinematic GPS positions were used to generate velocities, using equation (7) with an appropriate time interval, and these velocities compared with video timing velocities. We could use the filtered positions (from the Kalman filter) to generate another set of velocities, using (7) which would probability yield a smoother velocity curve than the filtered curve in Figure 14. We have not done this in this paper.

CONCLUSION

In this paper, we have presented a detailed description of the sailing courses at Shallow Inlet for the recent attempt on the World Sailing Speed Record and the survey work involved in setting out the courses. The original set out of the reference pegs for the course transit posts used traditional survey techniques; Total Station radiations from reference marks with precision estimates of ±0.010 metres based on manufacturers accuracy statements. These assumptions were confirmed by a rapid static GPS survey of a substantial number of the original reference pegs that lends weight to our estimate of the accuracy of an individual sailing course defined by transit posts. We believe that by setting out course lengths of 500.3 metres there is a reasonable guarantee that the yacht will have travelled at least 500 metres between transits; ensuring that the ISAF/WSSRC rules are complied with.

To test the possibility of GPS derived velocities as an alternative to video derived velocities we mounted a GPS receiver on a powerboat and simulated three runs over the sailing courses gathering 12,280 kinematic GPS positions at 0.1 second intervals. This data was analysed in three different ways.

(1) Velocity plots.
   Successive positions yield distance travelled, which divided by the time interval, gives an approximation of the instantaneous velocity. We have demonstrated that this crude estimation of velocity can be improved by increasing the time interval between sampling points by using equation (7). The appropriate time interval for a desired precision of velocity can be determined by equation (9). The resulting velocity plots are not useful for determining average velocity to an acceptable degree of accuracy, but they may be used as a means of identifying time intervals requiring further examination.

(2) Kinematic GPS positions and derived velocity.
   In our analysis, we have shown that two plausible *average velocities* can be derived from kinematic GPS positions. The first $A_1(V)$ is determined by equation (9) and is based on theorems of integral calculus using velocities calculated from equation (7). This average takes into account the actual distance travelled by the yacht and on a curved course such as the Shallow Inlet courses, this might be significantly different from the chord distance between transit lines. The second average $A_2(V)$ is determined from the chord distance between appropriate measurement epochs. The chord distance travelled can be used to calculate a time, corrected to precisely 500 metres as per the ISAF/WSSRC rules.

   The second average velocities compared favourably with those derived using the video technique approved by the ISAF/WSSRC.

(3) Positions and velocities from a Kalman filter.
   A Kalman filter is a well-documented procedure for determining the state (position, velocity and acceleration) of a dynamic system and the precision of filtered quantities. We have set out the Kalman filter equations and demonstrated that with appropriate estimates of precision and a properly constructed dynamic model, filtered velocities are in close agreement with those obtained by equation (7). This gives us confidence in average velocities obtained from kinematic GPS.

We believe that kinematic GPS is a viable alternative to the currently acceptable video technique for determining the average velocity of a yacht attempting to set a sailing speed record. GPS has a significant advantage over the transit post method in that a yacht is not confined to a fixed course; it may sail in any direction determined by the current wind direction and sea-state. Our tests demonstrate that kinematic GPS provides coordinates with a precision of ±0.010 m or better, at regular and precise time intervals, which can be used to determine chord distances between measurement epochs and distance travelled. These distances yield average velocities (i) over "exact" distances travelled or (ii) over chords, which can be corrected to times over exactly 500 metres.

We hope that the information contained in this paper may be of use to the Macquarie Speed Sailing Team in future record attempts. The authors would like to acknowledge the help provided by the members of the Macquarie Speed Sailing Team, both in the preparation of data for this paper and for their assistance during the field trials.

REFERENCES

Apostol, T., 1967. *Calculus,* Blaisdell Publishing Co., London.

Brown, R.G. and P.Y.C. Hwang, 1992. *Introduction to Random Signals and Applied Kalman Filtering,* 2nd ed, John Wiley & Sons, Inc.

Bruton, A.M., C.L. Glennie and K.P. Schwarz, 1999. 'Differentiation for high-precision GPS velocity and acceleration determination', *GPS Solutions,* Vol. 2, No. 4, pp. 7-21.

Dahlquist, G and A. Björk, 1974. *Numerical Methods,* Prentice-Hall, London.

Herbert, Capt. J., J. Keith, S. Ryan, M. Szarmes, G. Lachapelle and M.E. Cannon, 1997. 'DGPS kinematic carrier phase signal simulation analysis for precise aircraft velocity determination', *Proceedings of the Institute of Navigation (ION) Annual Meeting,* Alburquerque, New Mexico, 3 June – 2 July, 1997.

ISAF, 2002. International Sailing Federation, http://www.sailing.org/. Accessed 24 March 2002.

Kalman, R.E., 1960. 'A new approach to linear filtering and prediction problems', Transactions of the American Society of Mechanical Engineers (ASME) *Journal of Basic Engineering,* Vol. 82D, pp. 35-45, Mar. 1960.

Parkinson, B.W. and J.J. Spilker Jr. (eds), 1996. *Global Positioning System: Theory and Applications Vols I and II,* Volume 164 of Progress in Astronautics and Aeronautics, Paul Zarchan (Ed in Chief), American Institute of Aeronautics and Astronautics Inc, Washington DC.

Ryan, S., G. Lachapelle and M.E. Cannon, 1997. 'DGPS kinematic carrier phase signal simulation analysis in the velocity domain', *Proceedings of the Institute of Navigation (ION) GPS 97,* Missouri, September 16-19, 1997.

Sorenson, H.W., 1970. 'Least-squares estimation from Gauss to Kalman', *IEEE Spectrum,* Vol. 7, pp. 63-68, July 1970.

WSSRC, 2002. World Sailing Speed Record Council, http://www.sailspeedrecords.com/rulesinshore.html. Accessed 24 March 2002.

Zarchan, P. and H. Musoff, 2000. *Fundamentals of Kalman Filtering: A Practical Approach,* Volume 190 of Progress in Astronautics and Aeronautics, Paul Zarchan (Ed in Chief), American Institute of Aeronautics and Astronautics Inc, Reston, Virginia.

APPENDIX A

THE KALMAN FILTER

A Kalman filter is a set of mathematical equations that are applied recursively to estimate the state of a dynamic system. In our case, the dynamic system is the powerboat (with GPS receiver) moving along the course. It receives position at time t_{k-1}, East and North (*E,N*) coordinates from kinematic GPS measurements (the *primary* measurement model), and moves to position t_k, according to a *dynamic* model, where it receives new position information. The state of the system at t_k is its position E_k, N_k, its velocity $\dot{E}_k, \dot{N}_k$ and acceleration $\ddot{E}_k, \ddot{N}_k$ written as the $(u,1)$ *state vector* $\mathbf{x}_k$; *u* being the number of unknowns which in our case is six

$$\hat{\mathbf{x}}_k = \begin{bmatrix} E \\ N \\ \dot{E} \\ \dot{N} \\ \ddot{E} \\ \ddot{N} \end{bmatrix}_k \tag{A1}$$

The "hat" symbol (^) above the vector **x** indicates that it is an estimate of the true (but unknown) state of the system derived from the Kalman filter.

A Kalman filter takes an initial estimate of the state vector $\hat{\mathbf{x}}$ and the state cofactor matrix (estimates of precisions) $\mathbf{Q}_x$ at t_{k-1} and predicts $\mathbf{x}'$ and $\mathbf{Q}'_x$ at t_k according to the dynamic model and its associated cofactor matrix. It then updates the predicted quantities using the measurements at t_k and the measurement cofactor matrix, producing new estimates $\hat{\mathbf{x}}$ and $\mathbf{Q}_x$. This process is repeated for successive measurements.

The *primary* measurement model has the general form

$$\mathbf{l}_k + \mathbf{v}_k = \hat{\mathbf{l}}_k \tag{A2}$$

$\mathbf{l}_k$ is the $(n,1)$ vector of measurements, $\mathbf{v}_k$ is an $(n,1)$ vector of residuals (small unknown corrections to the measurements) and $\hat{\mathbf{l}}_k$ are estimates of the true (but unknown) measurements. *n* is the number of measurements, which in our case is two.

The primary model can be expressed in terms of the state vector as

$$\mathbf{v}_k + \mathbf{B}_k \hat{\mathbf{x}}_k = -\mathbf{l}_k \tag{A4}$$

or

$$\begin{bmatrix} v_E \\ v_N \end{bmatrix}_k + \begin{bmatrix} -1 & 0 & 0 & 0 & 0 & 0 \\ 0 & -1 & 0 & 0 & 0 & 0 \end{bmatrix} \begin{bmatrix} E \\ N \\ \dot{E} \\ \dot{N} \\ \ddot{E} \\ \ddot{N} \end{bmatrix}_k = -\begin{bmatrix} E_{obs} \\ N_{obs} \end{bmatrix}_k$$

$\mathbf{B}_k$ is an (n,u) coefficient matrix and $\mathbf{l}_k$ is a $(u,1)$ vector of observations.

The *dynamic* model linking the state of the system at time t_{k-1} with its state at t_k is

$$\hat{\mathbf{x}}_k = \mathbf{T}\hat{\mathbf{x}}_{k-1} + \mathbf{v}_m \qquad (A5)$$

$\mathbf{T}$ is the (u,u) *Transition matrix* which models the dynamic relationships between the states at t_{k-1} and t_k.

$\mathbf{v}_m$ is a $(u,1)$ vector of residuals (small unknown corrections) reflecting the fact that the dynamic model is only an approximation of the true (but unknown) model linking the states at t_{k-1} and t_k.

The elements of the transition matrix are obtained from the dynamic equations linking position, velocity and acceleration

$$
\begin{aligned}
E_k &= E_{k-1} + \dot{E}_{k-1}\,\Delta t + \tfrac{1}{2}\ddot{E}_{k-1}\,\Delta t^2 \\
N_k &= N_{k-1} + \dot{N}_{k-1}\,\Delta t + \tfrac{1}{2}\ddot{N}_{k-1}\,\Delta t^2 \\
\dot{E}_k &= \dot{E}_{k-1} + \ddot{E}_{k-1}\,\Delta t \\
\dot{N}_k &= \dot{N}_{k-1} + \ddot{N}_{k-1}\,\Delta t \\
\ddot{E}_k &= \ddot{E}_{k-1} \\
\ddot{N}_k &= \ddot{N}_{k-1}
\end{aligned}
\qquad (A6)
$$

and (A5) can be written as

$$
\begin{bmatrix} E \\ N \\ \dot{E} \\ \dot{N} \\ \ddot{E} \\ \ddot{N} \end{bmatrix}_k
=
\begin{bmatrix}
1 & 0 & \Delta t & 0 & \tfrac{1}{2}\Delta t^2 & 0 \\
0 & 1 & 0 & \Delta t & 0 & \tfrac{1}{2}\Delta t^2 \\
0 & 0 & 1 & 0 & \Delta t & 0 \\
0 & 0 & 0 & 1 & 0 & \Delta t \\
0 & 0 & 0 & 0 & 1 & 0 \\
0 & 0 & 0 & 0 & 0 & 1
\end{bmatrix}
\begin{bmatrix} E \\ N \\ \dot{E} \\ \dot{N} \\ \ddot{E} \\ \ddot{N} \end{bmatrix}_{k-1}
+ \mathbf{v}_m
\qquad (A7)
$$

The elements of the vector of model corrections $\mathbf{v}_m$ can be considered as derivatives (differential ratios) expressed as functions of the unknown but random rate of change of accelerations $d\ddot{E}/dt$ and $d\ddot{N}/dt$ known as *jerk* and having units $\mathrm{m/s^3}$.

$$
\mathbf{v}_m =
\begin{bmatrix} dE/dt \\ dN/dt \\ d\dot{E}/dt \\ d\dot{N}/dt \\ d\ddot{E}/dt \\ d\ddot{N}/dt \end{bmatrix}
= \mathbf{Hw} =
\begin{bmatrix}
dE/d\ddot{E} & 0 \\
0 & dN/d\ddot{N} \\
d\dot{E}/d\ddot{E} & 0 \\
0 & d\dot{N}/d\ddot{N} \\
1 & 0 \\
0 & 1
\end{bmatrix}
\begin{bmatrix} d\ddot{E}/dt \\ d\ddot{N}/dt \end{bmatrix}
\qquad (A8)
$$

$\mathbf{H}$ is a (u,n) coefficient matrix and the $(n,1)$ vector $\mathbf{w}$ is the *system driving noise.* The elements of $\mathbf{H}$ can be determined by differentiating equations (A6) giving

$$dE/d\ddot{E} = \tfrac{1}{2}\Delta t^2, \quad dN/d\ddot{N} = \tfrac{1}{2}\Delta t^2, \quad d\dot{E}/d\ddot{E} = \Delta t \quad \text{and} \quad d\dot{N}/d\ddot{N} = \Delta t$$

and the vector of model corrections is

$$\mathbf{v}_m = \mathbf{H}\,\mathbf{w} = \begin{bmatrix} \frac{1}{2}\Delta t^2 & 0 \\ 0 & \frac{1}{2}\Delta t^2 \\ \Delta t & 0 \\ 0 & \Delta t \\ 1 & 0 \\ 0 & 1 \end{bmatrix} \begin{bmatrix} d\ddot{E}/dt \\ d\ddot{N}/dt \end{bmatrix} \tag{A9}$$

The primary model and the dynamic model have associated *cofactor matrices* $\mathbf{Q}$ and $\mathbf{Q}_m$ that contain estimates of the precision of the measurements and the dynamic model corrections respectively.

$\mathbf{Q}$ is the (n,n) cofactor matrix of the measurements in the primary model

$$\mathbf{Q} = \begin{bmatrix} s_E^2 & s_{EN} \\ s_{EN} & s_N^2 \end{bmatrix} \tag{A10}$$

$s_E^2 = s_N^2$ are estimates of the variances of the kinematic GPS coordinates. s_{EN} is an estimate of the covariance between the E and N coordinates. In our case we consider that the E and N coordinates are independent random variables and $s_{EN} = 0$.

$\mathbf{Q}_m$ is the (u,u) cofactor matrix of the of the dynamic model corrections and is obtained by applying the general law of propagation of variances to equation (A9) giving

$$\mathbf{Q}_m = \mathbf{H}\mathbf{Q}_w\mathbf{H}^T \tag{A11}$$

$\mathbf{Q}_w$ is the (n,n) cofactor matrix of the system driving noise containing estimates of the variance of the rate of change of acceleration (the jerk).

$$\mathbf{Q}_m = \begin{bmatrix} \frac{1}{2}\Delta t^2 & 0 \\ 0 & \frac{1}{2}\Delta t^2 \\ \Delta t & 0 \\ 0 & \Delta t \\ 1 & 0 \\ 0 & 1 \end{bmatrix} \begin{bmatrix} s_{\ddot{E}}^2 & 0 \\ 0 & s_{\ddot{N}}^2 \end{bmatrix} \begin{bmatrix} \frac{1}{2}\Delta t^2 & 0 & \Delta t & 0 & 1 & 0 \\ 0 & \frac{1}{2}\Delta t^2 & 0 & \Delta t & 0 & 1 \end{bmatrix} \tag{A12}$$

The Kalman filter equations provide the (u,u) cofactor matrix $\mathbf{Q}_x$ containing estimates of the precisions of the elements of the state vector

$$\mathbf{Q}_x = \begin{bmatrix} s_E^2 & s_{EN} & s_{E\dot{E}} & s_{E\dot{N}} & s_{E\ddot{E}} & s_{E\ddot{N}} \\ s_{EN} & s_N^2 & s_{N\dot{E}} & s_{N\dot{N}} & s_{N\ddot{E}} & s_{N\ddot{N}} \\ s_{E\dot{E}} & s_{N\dot{E}} & s_{\dot{E}}^2 & s_{\dot{E}\dot{N}} & s_{\dot{E}\ddot{E}} & s_{\dot{E}\ddot{N}} \\ s_{E\dot{N}} & s_{N\dot{N}} & s_{\dot{E}\dot{N}} & s_{\dot{N}}^2 & s_{\dot{N}\ddot{E}} & s_{\dot{N}\ddot{N}} \\ s_{E\ddot{E}} & s_{N\ddot{E}} & s_{\dot{E}\ddot{E}} & s_{\dot{N}\ddot{E}} & s_{\ddot{E}}^2 & s_{\ddot{E}\ddot{N}} \\ s_{E\ddot{N}} & s_{N\ddot{N}} & s_{\dot{E}\ddot{N}} & s_{\dot{N}\ddot{N}} & s_{\ddot{E}\ddot{N}} & s_{\ddot{N}}^2 \end{bmatrix} \tag{A13}$$

All the elements of the primary and the dynamic models have been defined as well as the cofactor matrices associated with both. The primary model at t_{k-1} and t_k, and the dynamic model linking the states at t_{k-1} and t_k give rise to the system of equations

$$\mathbf{A}_{k-1}\mathbf{v}_{k-1} + \mathbf{B}_{k-1}\mathbf{x}_{k-1} = \mathbf{l}_{k-1}$$
$$\mathbf{A}_k\mathbf{v}_k + \mathbf{B}_k\mathbf{x}_k = \mathbf{l}_k \tag{A14}$$
$$\mathbf{x}_k = \mathbf{T}\mathbf{x}_{k-1} + \mathbf{v}_m$$

Note that in our case $\mathbf{A} = \mathbf{I}$ where $\mathbf{I}$ is the Identity matrix. Enforcing the least squares condition that the sum of the squares of the residuals be a minimum, gives rise to a set of recursive equations (the Kalman Filter) which are applied as follows.

With initial estimates of the state vector $\hat{\mathbf{x}}_{k-1}$ and the cofactor matrix $\mathbf{Q}_{x_{k-1}}$ a Kalman Filter has the following five general steps

(1)   Project the state forward to give approximate values at t_k

$$\mathbf{x}'_k = \mathbf{T}\hat{\mathbf{x}}_{k-1}$$

(2)   Project the state cofactor matrix forward

$$\mathbf{Q}'_{x_k} = \mathbf{T}\mathbf{Q}_{x_{k-1}}\mathbf{T}^T + \mathbf{Q}_m$$

(3)   Compute the Kalman *Gain matrix*

$$\mathbf{K} = \mathbf{Q}'_{x_k}\mathbf{B}_k^T\left(\mathbf{Q} + \mathbf{B}_k\mathbf{Q}'_{x_k}\mathbf{B}_k^T\right)^{-1}$$

(4)   Update the estimate with the measurements at t_k

$$\hat{\mathbf{x}}_k = \mathbf{x}'_k + \mathbf{K}_k\left(\mathbf{l}_k - \mathbf{B}_k\mathbf{x}'_k\right)$$

(5)   Update the state cofactor matrix

$$\mathbf{Q}_{x_k} = \left(\mathbf{I} - \mathbf{K}_k\mathbf{B}_k\right)\mathbf{Q}'_{x_k}\left(\mathbf{I} - \mathbf{K}_k\mathbf{B}_k\right)^T + \mathbf{K}_k\mathbf{A}\mathbf{Q}\mathbf{A}\mathbf{K}_k^T$$
$$= \left(\mathbf{I} - \mathbf{K}_k\mathbf{B}_k\right)\mathbf{Q}'_{x_k}$$

Go to step (1) and repeat the process for the next measurement epoch.

In the section below, a detailed description of the steps in a Kalman filter as implemented in a computer program are set out

---

Step 1   Set the elements of the transition matrix

$$\mathbf{T} = \begin{bmatrix} 1 & 0 & \Delta t & 0 & \frac{1}{2}\Delta t^2 & 0 \\ 0 & 1 & 0 & \Delta t & 0 & \frac{1}{2}\Delta t^2 \\ 0 & 0 & 1 & 0 & \Delta t & 0 \\ 0 & 0 & 0 & 1 & 0 & \Delta t \\ 0 & 0 & 0 & 0 & 1 & 0 \\ 0 & 0 & 0 & 0 & 0 & 1 \end{bmatrix}$$

Step 2   Set the cofactor matrix of the system driving noise

$$\mathbf{Q}_w = \begin{bmatrix} s_{\ddot{E}}^2 & 0 \\ 0 & s_{\ddot{N}}^2 \end{bmatrix}$$

Step 3 Set the coefficient matrix of the system driving noise

$$\mathbf{H} = \begin{bmatrix} \frac{1}{2}\Delta t^2 & 0 \\ 0 & \frac{1}{2}\Delta t^2 \\ \Delta t & 0 \\ 0 & \Delta t \\ 1 & 0 \\ 0 & 1 \end{bmatrix}$$

Step 4 Compute the cofactor matrix of the dynamic model

$$\mathbf{Q}_m = \mathbf{H}\mathbf{Q}_w\mathbf{H}^T$$

Step 5 Set the counter

$$k = 1$$

Step 6 Set the starting estimates of the state vector

$$\hat{\mathbf{x}}_k = \begin{bmatrix} E \\ N \\ \dot{E} \\ \dot{N} \\ \ddot{E} \\ \ddot{N} \end{bmatrix}_k$$

Note that estimates of the starting velocities and accelerations can be computed from kinematic GPS coordinates at epochs 1, 2 and 3

Step 7 Set the starting estimates of the state cofactor matrix

$$\mathbf{Q}_{x_k} = \begin{bmatrix} s_E^2 & 0 & 0 & 0 & 0 & 0 \\ 0 & s_N^2 & 0 & 0 & 0 & 0 \\ 0 & 0 & s_{\dot{E}}^2 & 0 & 0 & 0 \\ 0 & 0 & 0 & s_{\dot{N}}^2 & 0 & 0 \\ 0 & 0 & 0 & 0 & s_{\ddot{E}}^2 & 0 \\ 0 & 0 & 0 & 0 & 0 & s_{\ddot{N}}^2 \end{bmatrix}_k$$

Note that at this step the estimates of the covariances are all set to zero.

Step 8 Increment the counter

$$k = k + 1$$

Step 9 Compute the predicted state vector

$$\mathbf{x}'_k = \begin{bmatrix} E' \\ N' \\ \dot{E}' \\ \dot{N}' \\ \ddot{E}' \\ \ddot{N}' \end{bmatrix}_k = \begin{bmatrix} 1 & 0 & \Delta t & 0 & \frac{1}{2}\Delta t^2 & 0 \\ 0 & 1 & 0 & \Delta t & 0 & \frac{1}{2}\Delta t^2 \\ 0 & 0 & 1 & 0 & \Delta t & 0 \\ 0 & 0 & 0 & 1 & 0 & \Delta t \\ 0 & 0 & 0 & 0 & 1 & 0 \\ 0 & 0 & 0 & 0 & 0 & 1 \end{bmatrix} \begin{bmatrix} E \\ N \\ \dot{E} \\ \dot{N} \\ \ddot{E} \\ \ddot{N} \end{bmatrix}_{k-1}$$

Step 10 Compute the predicted state cofactor matrix

$$\mathbf{Q}'_{x_k} = \mathbf{T}\mathbf{Q}_{x_{k-1}}\mathbf{T}^T + \mathbf{Q}_m$$

Step 11 Set the elements of the coefficient matrix of the primary model

$$\mathbf{B} = \begin{bmatrix} -1 & 0 & 0 & 0 & 0 & 0 \\ 0 & -1 & 0 & 0 & 0 & 0 \end{bmatrix}$$

Step 12 Compute the numeric terms of the primary model

$$\mathbf{f}_k = \begin{bmatrix} E' - E_{obs} \\ N' - N_{obs} \end{bmatrix}_k$$

Step 13 Compute the Kalman *Gain matrix*

$$\mathbf{K}_k = \mathbf{Q}'_{x_k}\mathbf{B}_k^T\left(\mathbf{Q} + \mathbf{B}_k\mathbf{Q}'_{x_k}\mathbf{B}_k^T\right)^{-1}$$

Step 14 Compute corrections to the state vector

$$\Delta\mathbf{x}_k = \mathbf{K}_k\left(\mathbf{l}_k - \mathbf{B}_k\mathbf{x}'_k\right) = \mathbf{K}_k\mathbf{f}_k$$

Step 15 Compute the new estimate of the state vector

$$\mathbf{x}_k = \mathbf{x}'_k + \Delta\mathbf{x}_k$$

Step 16 Compute the cofactor *Update matrix*

$$\mathbf{U}_k = \mathbf{I} - \mathbf{K}_k\mathbf{B}_k$$

Note that **I** is the identity matrix

Step 17 Compute the new estimate of the state cofactor matrix

$$\mathbf{Q}_{x_k} = \mathbf{U}\mathbf{Q}'_{x_k}$$

Go To Step 8